

Variability of the Arctic Frontal Zone Characteristics in the Barents and Kara Seas in the First Two Decades of the XXI Century

A. A. Konik ^{1,2} ✉, A. V. Zimin ^{1,2}

¹ P. P. Shirshov Institute of Oceanology, Russian Academy of Sciences, Saint-Petersburg, Russian Federation

² Saint Petersburg State University, Saint-Petersburg, Russian Federation
✉ konikrshu@gmail.com

Abstract

Purpose. The article is devoted to studying the long-term variability of the characteristics of surface manifestations of the Arctic Frontal Zone formed seasonally in the Marginal Ice Zone of the Arctic seas.

Methods and Results. To identify the frontal zone, the satellite measurements of surface temperature carried out by the MODIS/Aqua and VIIRS/Suomi NPP from August to September 2002–2020 are used as initial data. The Arctic Frontal Zone position and characteristics were determined using the cluster analysis. In the warm period of the year, the average long-term thermal surface gradient in the Arctic Frontal Zone is revealed to be 0.06 °C/km, and its area – 348,000 km². Variability of the interannual gradient estimates in this region ranged from 0.04 to 0.09 °C/km, and the area – from 159,000 to 489,000 km².

Conclusions. During the last two decades, spatial position of the frontal zone has been characterized by a significant shift to the north (81°–82°N). The surface temperature in the frontal zone in the last decade was on average higher than that in the previous one. Such dynamics is conditioned by retreat of the arctic ice cover edge. The thermal gradient maximum values in the Arctic Frontal Zone were recorded in 2009, 2016 and 2018 at the significant near-surface wind speeds and the reduced ice cover concentration. The surface temperature, the thermal gradient and the frontal zone area are shown to be conditioned by the ice area and concentration in last year's autumn season. It is established that during a warm season, the North Atlantic Oscillation winter index governs variation of the surface temperature in the Arctic Frontal Zone.

Keywords: Arctic zone, frontal zone, marginal ice zone, ice cover, satellite measurements, NAO, Barents Sea, Kara Sea

Acknowledgements: The study was carried out within the framework of the RFBR grant No. 20–35–90053 and state assignment of IO RAS on theme FMWE–2021–0014.

For citation: Konik, A.A. and Zimin, A.V., 2022. Variability of the Arctic Frontal Zone Characteristics in the Barents and Kara Seas in the First Two Decades of the XXI Century. *Physical Oceanography*, 29(6), pp. 659–673. doi:10.22449/1573-160X-2022-6-659-673

DOI: 10.22449/1573-160X-2022-6-659-673

© A. A. Konik, A. V. Zimin, 2022

© Physical Oceanography, 2022

1. Introduction

The Arctic ice pack is one of the most important characteristics of the polar regions. The characteristics and spatial dynamics of ice affect both the regional features of individual seas [1] and the entire climatic system of the Arctic [2]. In recent decades, an intensive retreat of the ice cover edge towards the North Pole has been observed in the Arctic region [3, 4]. On the boundary of the first-year ice and completely open sea waters, a Marginal Ice Zone (MIZ) that is unique in its



hydrological structure is formed (works ¹ and [5–9]). The processes of interaction between the ocean and the atmosphere with sea ice in the MIZ enhance small-scale turbulence and convective mixing [5, 6], and also affect various marine food chains [10, 11].

Numerous studies of the MIZ [10–16] revealed that as a result of the interaction of relatively cold freshened waters near the ice cover edge and warmer sea waters farther from the edge, a frontal zone is formed [13]. To date, this zone has no established name. It is known that in some studies it is called the Arctic [12, 13], Near-Edge [17], or Frontal zone of the MIZ [15]. In this paper, the authors will rely on the terminology of [13] and use the term “Arctic Frontal Zone” (AFZ).

The methodological difficulties of contact and remote observations in the AFZ cause the absence of any information about the long-term variability of quantitative estimates and its dynamics in the Barents and Kara Seas. It is known from individual works [13, 17] that in the Barents Sea, according to shipborne measurements, the AFZ has complex seasonal and interannual spatial dynamics, which depends on the characteristics and position of the ice cover edge, as well as surface wind parameters. In the warm period of the year, the AFZ in the Barents Sea [16, 17] is characterized by pronounced vertical and horizontal thermohaline gradients. Using satellite probing data from high-resolution radiometers, the spatial dynamics of the AFZ was described and some seasonal estimates of thermal gradients and the width of this zone were obtained in the Kara Sea in recent studies [14, 17].

However, very rare and fragmentary studies do not enable one to describe the spatial dynamics over a long-time interval and systematize quantitative estimates of the AFZ characteristics in the Barents and Kara Seas. Obtaining and refining these data is an important aspect in understanding ongoing global climate change. No less relevant is the study of the relationship between the characteristics of the AFZ and large-scale atmospheric circulation, which will make it possible to reveal the features of ocean-atmosphere interaction process in the northern parts of the Arctic seas.

Thus, the purpose of this study is the detection of the AFZ on the surface, the study of its interannual variability, and the analysis of estimates of its relationship with regional and global hydrometeorological processes.

2. Data and methods

The spatial variability and quantitative characteristics of the AFZ were estimated using monthly average satellite measurements of the sea surface temperature (SST) from August to September 2002–2020. To identify the AFZ, the data from satellites with high resolution infrared radiometers MODIS/Aqua and VIIRS/Suomi NPP were used. The spatial resolution of the data is 0.05° in latitude and longitude [18].

The characteristics and position of the AFZ were determined by joint analysis of the SST fields and their gradients. The thermal horizontal gradients were calculated according to the method presented in [19]. In the Matlab software, a two-

¹ Nikiforov, E.G. and Shpayher, A.O., 1980. [*Patterns of Formation of Large-Scale Fluctuations in the Hydrological Regime of the Arctic Ocean*]. Leningrad: Gidrometeoizdat, 270 p. (in Russian); Terziev, F.S., ed., 1990. *Hydrometeorology and Hydrochemistry of the Seas of the USSR. Volume 1. Barents Sea. Issue 1. Hydrometeorological Conditions*. Leningrad: Gidrometeoizdat, 280 p. (in Russian).

dimensional grid was created with coordinates from 75° to 83°N and 30° to 90°E in the Barents and Kara Seas with a step of 0.25° in latitude and longitude. Then the obtained data on the SST and its gradients were combined into a single matrix and interpolated to the specified grid.

The AFZ on the surface of the Barents and Kara Seas was identified in the Statistica 10 program using hierarchical and interactive cluster analysis algorithms² in two stages. In the first stage, the optimal number of classes was determined using the dendrograms constructed by the Ward method with the Euclidean metric. In the second stage, the final clustering was carried out using the *k*-means method. Based on the cluster analysis results, the distribution maps of the selected AFZ positions were constructed. The maps of the positions of the main water classes were analyzed for each individual month. For the subclass corresponding to the AFZ, the mean SST values, its gradients, and area were calculated on monthly and annual intervals, and the coordinates of the northernmost point of the frontal zone were determined. Further, on the basis of the obtained coordinates for decades, the frequency of latitudes was estimated, at which the northern boundary of the AFZ was recorded.

To analyze the wind effect on the AFZ parameters, we used 6-hour near-water wind velocity data from the ERA-Interim Reanalysis product, obtained from the website <https://www.ecmwf.int> from the European Center for Medium-Range Weather Forecasts (ECMWF). The wind field data were obtained from 2002 to 2019 and averaged to monthly values. The area and concentration (the term “concentration” is used in the initial data) of the ice cover in the study area was described using the data from the AMSR-E and AMSR-2 satellite radiometers. The data were prepared by the University of Bremen [20]. They also determined the ice cover edge position (on the maps presented in the work, these are the lines where the ice concentration was 1%) and the area of ice with different concentrations.

The analysis of the effect of global atmospheric processes on the change in the AFZ parameters was carried out using the NAO (North Atlantic Oscillation) atmospheric circulation index³, which reflects the intensity of zonal transport of air masses over the northern part of the Atlantic Ocean [21]. The data was downloaded from the Climate Prediction Center website (<https://www.cpc.ncep.noaa.gov>).

The cross-correlation analysis was applied to determine the degree of connection between the regional and global processes and the characteristics of the AFZ. The frontal zone characteristics were compared with data on the wind, area, and concentration of the ice cover on a monthly interval with a shift of up to 12 months. The data on atmospheric circulation indices correlated with the average seasonal estimates of the frontal zone characteristics over a time interval from 3 to 9 months. The obtained coefficients were tested for significance using Student’s *t*-test for a significance level of 95%.

² Vainovsky, P.A. and Malinin, V.N., 1992. [*Methods of Processing and Analysis of Oceanological Information: Multidimensional Analysis*]. St. Petersburg: RGGMI, 96 p. (in Russian).

³ Climate Prediction Center. 1999. *Climate Diagnostics Bulletin*. [online] Available at: https://www.cpc.ncep.noaa.gov/products/CDB/CDB_Archive_html/bulletin_0299/telemonc.gif [Accessed: 20 November 2022].

3. Results of the study

3.1. AFZ detection on the surface of the Barents and Kara seas. On the example of the results of temperature fields' clustering and its gradient by the Ward method, shown in Fig. 1, *a*, one can see two main classes, which are located quite far from each other. These classes can be attributed to clean sea waters and waters in the area of the Arctic ice pack. By reducing the threshold distance by more than three times, one can observe the division of the seawater class into two subclasses. According to general ideas about the characteristics of the Barents and Kara Sea waters (see works ⁴ and [22–24]), it is known that Arctic waters are observed in the region under consideration. During various studies [13, 14, 16], it was found that frontal zones of different genesis arise between the waters formed under the direct effect of the ice cover edge and the Arctic waters in this region. Accordingly, the results of clustering by the Ward method enable us to make an assumption about the presence of two modifications of sea waters in the surface layer and a separate class of waters in the area of the drifting ice pack. As a result, in this region, the allocation of three classes of water will be the most optimal from a physical and statistical point of view.

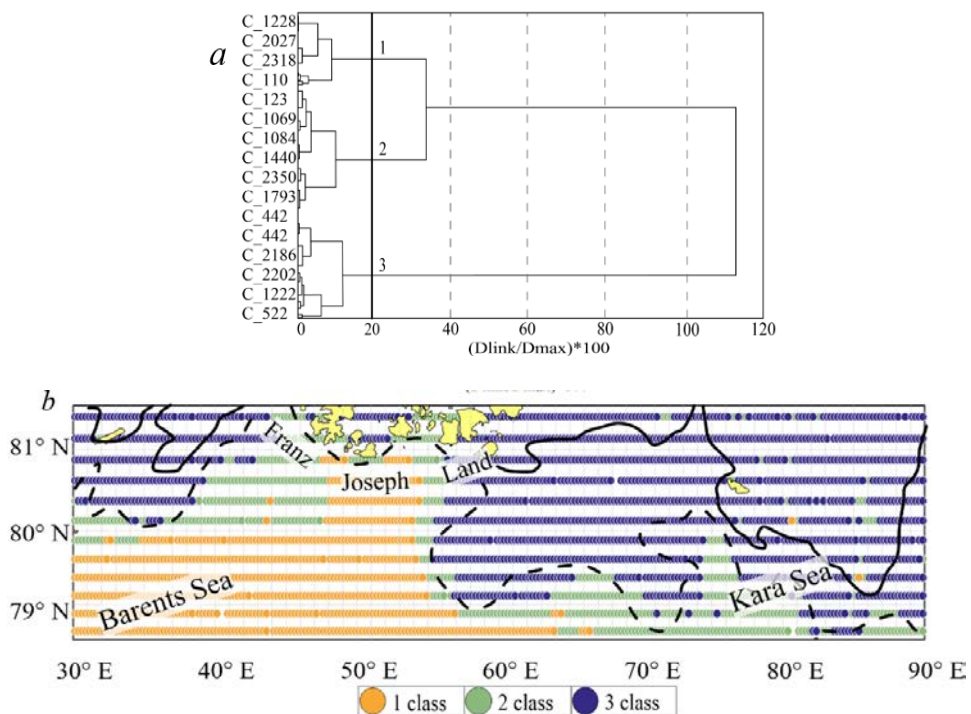


Fig. 1. Results of the cluster analysis and application of the satellite-derived ice parameters in August, 2002: *a* – dendrogram obtained by the Ward's method (black vertical line and numbers denote the water main classes); *b* – classification obtained by the *k*-means method (class 1 – arctic water mass; class 2 – AFZ; class 3 – waters in the ice cover area; black hatch line – the monthly average position of the ice cover edge (1% ice concentration); black solid line – boundary of the ice with 20% ice concentration)

⁴ Dobrovolsky, A.D. and Zalagin, B.S., 1982. *Seas of the USSR*. Moscow: MGU, 192 p. (in Russian).
662 PHYSICAL OCEANOGRAPHY VOL. 29 ISS. 6 (2022)

The resulting number of classes was applied in clustering by the *k*-means method, the results of which are represented in Fig. 1, *b*.

The quantitative estimates of the resulting clustering are presented in Table 1. It can be seen from the table that the classification provides clear correlation of the obtained classes with waters of different genesis, which are observed in the selected study region.

Table 1

Quantitative estimates of SST characteristics (\bar{T}), its gradients ($\nabla\bar{T}$) and AFZ area (s) based on the cluster analysis results for August, 2002

Class	\bar{T} , °C	$\nabla\bar{T}$, °C/km	$s \cdot 10^3$, km ²
1	2.6	0.03	272
2	1.8	0.06	263
3	-0.2	0.04	641

According to the studies (the works ⁵ and [9, 23–26]), the Arctic waters in the Barents and Kara Seas are most often observed above 77°–79°N and are located near Svalbard and Franz Joseph Land (FJL) archipelagos and ice cover edge. The position of the first class (see Fig. 1, *b*) generally corresponds to the climatic position of this water mass, described in the works ⁶ and in [23, 25]. The average temperature of the Arctic waters in the warm season averages 2–3 °C, which generally coincides with the clustering results (see Table 1).

The second class occupies a boundary position between the Arctic waters and the seasonal (melting) ice (concentration over 1%). The northern boundary of the class almost along its entire length is in contact with the ice cover edge. Such a spatial position of the class is comparable to the previously described position [13] of the AFZ at the ice boundary in the MIZ. This class has the maximum surface thermal gradient (0.06 °C/km) which, according to the classification ⁷, makes it possible to refer it to the frontal zone. An additional confirmation of the assignment of this class to the frontal zone is its minimum area (263,000 km²) in comparison with the area occupied by other classes. In addition, the results of expeditionary studies [16] correlate with the obtained value of the frontal zone thermal gradient,

⁵ Dobrovolsky, A.D. and Zalogin, B.S., 1982. *Seas of the USSR*. Moscow: MGU, 192 p. (in Russian); Vainovsky, P.A. and Malinin, V.N., 1992. [*Methods of Processing and Analysis of Oceanological Information: Multidimensional Analysis*]. St. Petersburg: RGGMI, 96 p. (in Russian).

⁶ Nikiforov, E.G. and Shpayher, A.O., 1980. [*Patterns of Formation of Large-Scale Fluctuations of the Hydrological Regime of the Arctic Ocean*]. Leningrad: Gidrometeoizdat, 270 p. (in Russian); Vainovsky, P.A. and Malinin, V.N., 1992. [*Methods of Processing and Analysis of Oceanological Information: Multidimensional Analysis*]. St. Petersburg: RGGMI, 96 p. (in Russian).

⁷ Fedorov, K.N., 1983. *The Physical Nature and Structure of Oceanic Fronts*. Berlin: Springer, 333 p. doi:10.1029/LN019

which was identified at the MIZ boundary. Based on the performed analysis, this class can be attributed to the AFZ.

An analysis of the AMSR-E radiometer data for August 2002 showed that in the 3rd class area, the maximum area (more than 340,000 km²) is occupied by waters with ice fields with a concentration of more than 1%. The quantitative SST estimates obtained as a result of clustering (mostly negative values) also confirm that this class belongs to waters in the area of seasonal ice fields (see Table 1). It should be noted that negative temperatures, similar to the temperature of surface waters, also form in separate open areas of thin ice near thawed patches.

Thus, as part of the clustering in the study area of the Barents and Kara Seas, it was possible to distinguish three classes: arctic waters, the AFZ, and waters in the area of seasonal ice fields.

3.2. Long-term and interannual variability of AFZ. The cluster analysis provided long-term quantitative estimates and describe the dynamics of the AFZ variability from 2002 to 2020. Table 2 shows the averaged long-term AFZ parameters for August and September.

Table 2

Average long-term estimates of SST (\bar{T}), its gradients ($\nabla\bar{T}$) and the AFZ area (s) for August and September

Month	\bar{T} , °C	$\nabla\bar{T}$, °C/km	$s \cdot 10^3$, km ²
August	1.2		364
September	0.8	0.06	332
Average	1.0		348

The long-term SST estimates for each month reflect the variation with a maximum in August and a minimum in September. The thermal gradient in August and September remains unchanged. The maximum area of the surface AFZ is recorded in August, and then a slight decrease in its value takes place.

An analysis of the long-term spatial dynamics of the AFZ (Fig. 2, *a – b*) revealed that in August the frontal zone is located in areas from 78°–80°N, being located southward of FJL archipelago. In September, the AFZ, dividing into two separate parts, shifts to the region of 80°–81°N. Probably, the main contribution to the variability of the frontal zone spatial position in a given period of the year is made by the intensity of solar radiation, which affects the melting and retreat of the ice cover edge to the north.

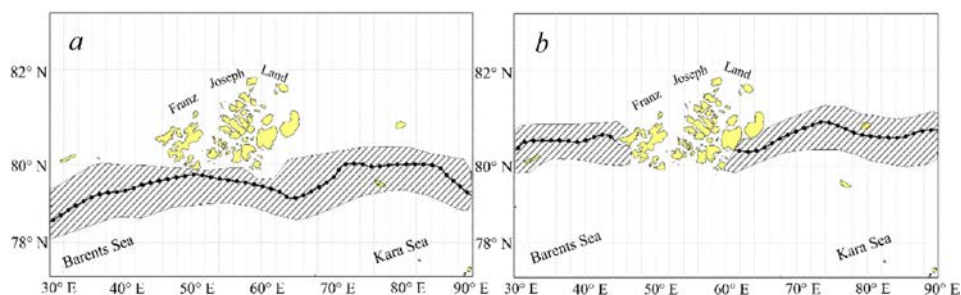


Fig. 2. Long-term AFZ positions (hatch lines area): *a* – August; *b* – September. Black line indicates position of the ice cover edge (1% ice concentration based on the AMSR-E and AMSR-2 radiometers data)

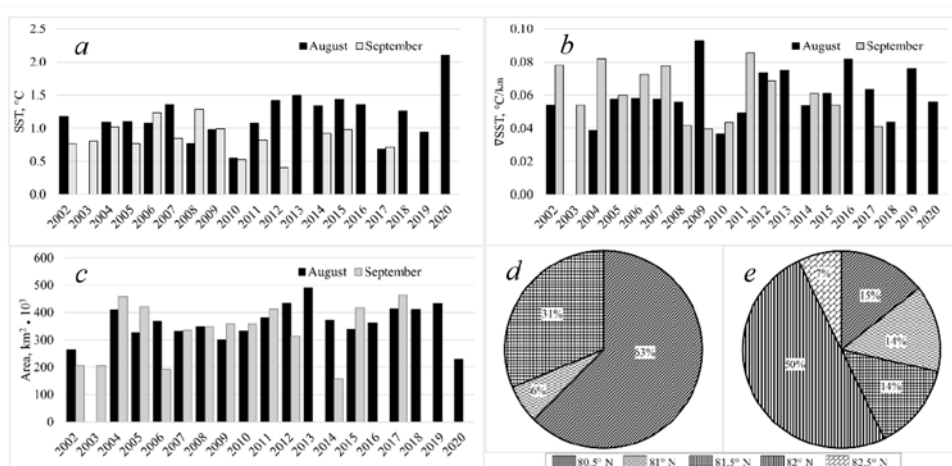


Fig. 3. Interannual variability (2002–2020) of SST (*a*), SST gradient (*b*), AFZ area (*c*) and repeatability of the coordinates of the zone northern boundary in 2002–2010 (*d*) and in 2011–2020 (*e*)

The interannual variability of temperature characteristics in the frontal zone for the entire study period is demonstrated in Fig. 3, *a*. It can be seen that from 2002 to 2020 the SST fluctuates from 0.4 °C in September to 2.1 °C in August. Most often, the maximum surface temperature is observed in August, and the minimum – in September. In the period from 2002 to 2012, the SST in the AFZ did not change significantly, and the maximum values reached 1.4 °C, which generally coincides with the average long-term estimates (see Table 2). In the second decade of the 21st century, a positive trend in surface temperature takes place, the maximum of which is observed in August 2020 and reaches 2.1 °C. This value is twice higher than the average estimates (see Table 2). It is important to immediately note that in recent years the AFZ in the region under consideration is registered only in August.

Variability of the value of the AFZ gradient from 2002 to 2020 (Fig. 3, *b*) is generally characterized by uniformity. The thermal gradient in the AFZ varies from 0.04 °C/km in 2010 to 0.09 °C/km in 2009. In the first decade of the 21st century

the magnitude of the SST gradient is almost unchanged and generally corresponds to its average long-term values (see Table 2). However, from 2011 to 2020, there is a slight increase in the thermal gradient with a maximum of 0.08 °C/km in September 2016. It should be noted that in certain months, for instance in August of 2009, 2016, 2019, at small SST values the maxima of SST gradient are observed in the AFZ. However, these cases are exceptional and do not apply to the entire study period.

The AFZ area parameters (Fig. 3, *c*) are characterized by a minimum value in September 2014 (139,000 km²) and a maximum in August 2013 (489,000 km²). The interannual variability of the area is characterized by insignificant fluctuations in the first decade of the 21st century (amplitude of 30–40,000 km²), and from 2010 to 2020 its range increases several times (amplitude of more than 330,000 km²). In some years, both positive (2004, 2013, 2017) and negative (2006, 2014, 2020) anomalies in the AFZ area are observed, their magnitude significantly exceeds the average long-term estimates (see Table 2). It is also worth noting the cycles of growth (2008–2012; 2016–2019) and decline (2004–2007; 2013–2015) of the area value, their interval is from 3 to 4 years.

An analysis of the frequency diagrams of the latitude of the AFZ northern boundary over 20 years (Fig. 3, *d–e*) showed that in the first decade the frontal zone was observed in the southern regions of FJL (80.5°–81.5°N), and in the second, it began to be observed more often much northwards, in the area up to 82.5°N. It is important to note that from 2010 to 2020, the percentage of occurrence of the frontal zone northern boundary at higher latitudes increased. Such a spatial position of the frontal zone is the main cause for the absence of its quantitative estimates in September in recent years. The AFZ, like the Arctic ice pack, is shifting significantly to the north and going far beyond the geographic boundaries of the Barents and Kara Seas.

3.3. Relationship of AFZ with regional and global hydrometeorological processes. Estimates of the characteristics of the area and ice cover concentration, as well as the characteristics of the near-water wind for the period under study in the considered water area, are presented in Fig. 4. The parameters of the area and concentration of the ice cover for the period under consideration have a pronounced negative time trend. At the same time, minimum estimates were more often recorded in certain years of the second decade of the 21st century (2012 – 117,000 km² and 5%, 2013 – 52,000 km² and 4%, 2018 – 110,000 km² and 3%, 2020 – 53,000 km² and 4%). It should be noted that the ice area in the studied region over the first two decades of the 21st century decreased on average by 200–250,000 km², and its density more than halved from 16 to 6%. The intensification of the wind impact was more often observed from 2002 to 2010: the maxima are observed in 2006 (2.9 m/s) and 2009 (3.5 m/s). In the second decade of the 21st century the wind velocity fell, in recent years its steady decrease has been taking place (2018 – 1.2 m/s, 2019 – 0.8 m/s). It is important to note that in recent years (from 2016 to 2019), the parameters of the ice cover and the average wind velocity have changed synchronously.

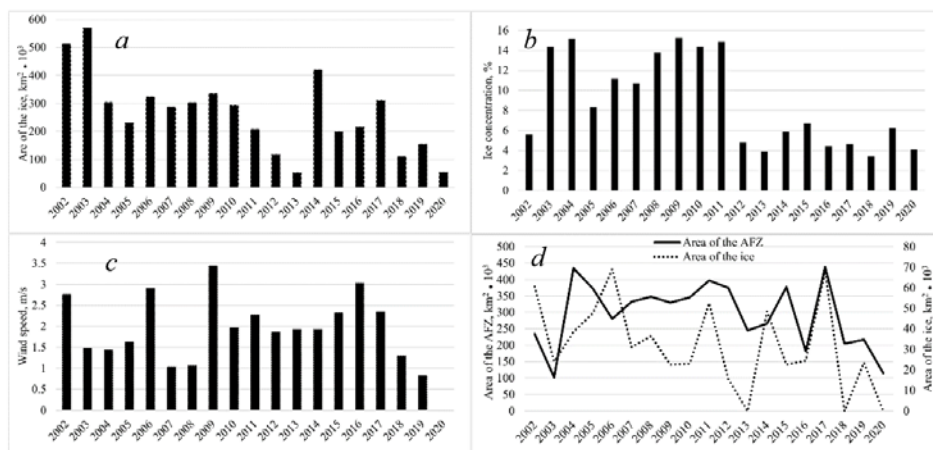


Fig. 4. Interannual estimates of the sea ice parameters for August and September, 2002–2020: *a* – ice cover area with a concentration from 1 to 100 %; *b* – average ice concentration in the region under study; *c* – near-surface wind speed; *d* – seasonal average values of the AFZ area and the ice cover one with a concentration from 1 to 20 %

A comparison of the interannual parameters of ice and wind with the AFZ characteristics showed that the overall increase in surface temperature in the frontal zone (see Fig. 3, *a*) for certain years (2015, 2016, 2018, 2020) is formed against the background of a low surface wind velocity, as well as a decrease in the area and concentration of the ice cover. Most of the small SST values in the AFZ (2002, 2003, 2007, 2009) coincide with the large area and concentration of ice and the maximum wind velocity in the region. The exception is 2012 minimum SST values (0.4 °C) and a small area and ice concentration are observed when at an average wind velocity of no more than 2 m/s. Probably at the beginning of the second decade of the 21st century an intense melting of ice could not have a one-time response in changing the AFZ surface temperature. However, the constant increase in the sea surface open from ice against the background of low wind velocities, apparently, affected the intensification of radiative heating and the formation of significant positive SST anomalies in the AFZ, for example, in August 2020.

A large value of the AFZ thermal gradient (see Fig. 3, *b*), recorded in 2009, 2016, and 2018, was observed at relatively high near-water wind velocities and minima in the area and concentration of the ice cover. The increase in the gradient probably occurs as a result of an increased inflow of cold freshened water into the area outside the ice zone due to ice melting. The melting accelerates due to the increase in near-water wind velocity. Small SST gradients in September 2008 and August – September 2010 correspond to a low wind velocity and periods of maxima in the area and concentration of ice, which indicates a relationship between the characteristics of the AFZ gradient and the volume of water incoming as a result of melting.

The maximum values of the AFZ area (2012, 2013, 2017, 2019) coincide with periods when low wind velocities and minima in the area and concentration of the ice cover are observed. The minimum areas occupied by AFZ are observed in the years of increased area and concentration of ice (2002, 2003, 2006, 2014), as well as wind

intensification (2009, 2016). Comparison of the area of the AFZ and the area of ice with a concentration of no more than 20% in the region under consideration (Fig. 4, *d*) showed their almost synchronous variability. This interdependence suggests that the intensity of ice melting makes a significant contribution to the formation of the AFZ area. The only exception (resynchronization) was recorded in 2006, when, with a decrease in the AFZ area, an increase in the ice area with its low concentration was observed, which was probably due to the intensification of the northern surface wind velocity during this period (Fig. 4, *a – c*) that affected the increase in the volume of ice carried out from the northern regions of the Arctic.

The role of the wind in changing the characteristics of the frontal zone is well illustrated in Fig. 5. The maximum AFZ area (Fig. 5, *a*), which is recorded in August 2013, is observed at northern winds with an average velocity of up to 3.5 m/s. In September 2014, at southerly winds with an average velocity of more than 4 m/s, the minimum AFZ area is recorded (Fig. 5, *b*).

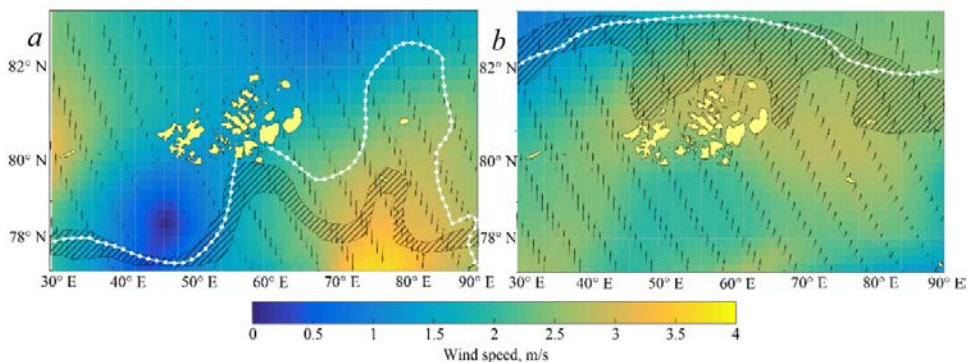


Fig. 5. Minimum (September, 2014) (*a*) and maximum (August, 2013) (*b*) areas of the AFZ propagation at various wind conditions. White line indicates the position of the ice cover edge

A correlation analysis of ice and AFZ parameters showed that ice concentration in the region under study for October of last year has a significant correlation coefficient with the SST gradient in August ($r = -0.44$) and the AFZ area in September ($r = 0.47$). In addition, the ice area in October of last year correlates with the September SST values in the AFZ ($r = 0.54$). A possible cause for such relationships lies in the heat reserve of waters formed at high latitudes during the warm season. As a result, in the next summer season, as the ice melts, the amount of released heat can affect the weakening of the gradient in the area of the frontal zone during its formation in August, and then in September affect the increase of SST and the AFZ area.

The AFZ parameters and NAO indices are applied to analyze the impact of global atmospheric transports, the interannual variation of which is demonstrated in Fig. 6.

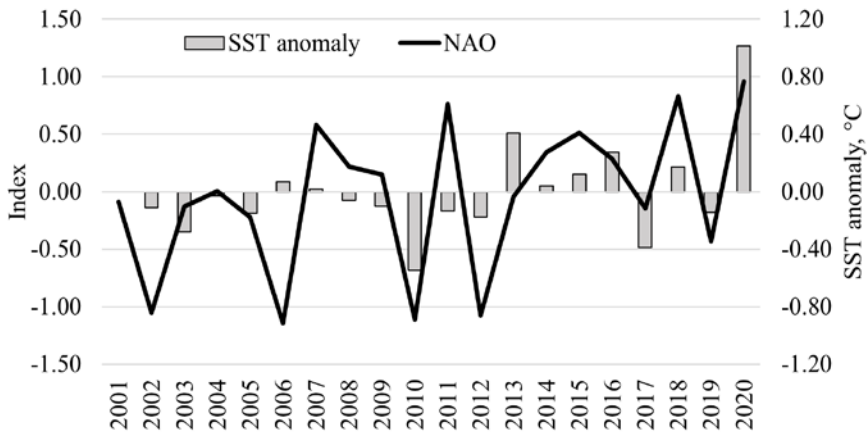


Fig. 6. Interannual dynamics of the averaged NAO indices in the winter season and the SST anomalies (differing from the SST average value in AFZ for the entire period under study) in AFZ for August and September

It is important to note that the values of the NAO index from 2011 to 2020 almost doubled compared to the first decade of the 21st century. Such a significant increase in the index in recent years indicates an intensification of the warm air zonal transfer from the northern part of the Atlantic Ocean to the considered area of the Barents and Kara Seas.

It is worth noting that positive NAO values are recorded during the periods of minor thermal anomalies. A correlation analysis of the NAO index winter values and the current summer SST values in the AFZ showed that there is a significant statistical relationship between them ($r = 0.50$). Probably, with the intensification of zonal transport from west to east in the winter season, there is an increase in the water transport from the North Atlantic to the Arctic. These processes affect the water temperature at the ice edge in the warm season, which can increase the SST in the AFZ. Let us note that the obtained absolute values of the correlation coefficients, although their value is small, show the importance of global transfers in the formation of the AFZ.

4. Conclusion

Within the framework of this study, an analysis of long-term spatial variability and quantitative estimates of characteristics in the AFZ area in the Barents and Kara Seas was carried out for the first time.

To detect the position and parameters of the AFZ, an approach based on cluster analysis on the integration of satellite data on surface temperature and its gradients was applied.

In this paper, we calculated and presented quantitative estimates of SSTs and their gradients in the AFZ for August and September 2002–2020. The long-term SST gradient in the frontal zone was 0.06 °C/km, and the area was 348,000 km². The interannual fluctuations in the thermal gradient ranged from 0.04 °C/km to 0.09 °C/km, and the AFZ area ranged from 159,000 to 489,000 km². At the same

time, a distinctive feature of this study is the description of the interannual variability of the surface AFZ under the changing climate of the Arctic. The surface temperature of the AFZ against the background of melting ice in the last decade has been growing rapidly, while the surface thermal gradient remains stable. The AFZ area is characterized by a cyclical growth/decline of its value with an interval of 3 to 4 years and generally correlates with the parameters of the area and concentration of ice. The analysis of the AFZ spatial position showed that in recent years the frontal zone has significantly shifted northward to the area of the Arctic Ocean open waters and is recorded in the Barents and Kara Seas only in August.

Based on estimates of the area and concentration of ice in the northern regions of the Barents and Kara Seas with a shift of 10 months, it is possible to assess the nature of the variability in estimates of surface temperature, its gradient, and the AFZ area. The variation of the NAO global atmospheric circulation winter indices can determine the change in the SST in the AFZ in the summer season. The obtained correlations can subsequently be used to create a predictive model that describes the characteristics of the AFZ area.

The following works will be aimed at studying the synoptic variability of the AFZ and creating a long-term forecast model for its main parameters.

REFERENCES

1. Kumar, A., Yadav, J. and Mohan, R., 2021. Spatio-Temporal Change and Variability of Barents- Kara Sea Ice, in the Arctic: Ocean and Atmospheric Implications. *Science of The Total Environment*, 753, 142046. doi:10.1016/j.scitotenv.2020.142046
2. Parkinson, C.L. and Cavalieri, D.J., 2008. Arctic Sea Ice Variability and Trends, 1979–2006. *Journal of Geophysical Research: Oceans*, 113(C7), C07003. doi:10.1029/2007jc004558
3. Maslanik, J., Stroeve, J., Fowler, C. and Emery, W., 2011. Distribution and Trends in Arctic Sea Ice Age through Spring 2011. *Geophysical Research Letters*, 38(13), L13502. doi:10.1029/2011gl047735
4. Serreze, M.C. and Stroeve, J., 2015. Arctic Sea Ice Trends, Variability and Implications for Seasonal Ice Forecasting. *Philosophical Transactions of the Royal Society A: Mathematical, Physical and Engineering Sciences*, 373(2045), 20140159. doi:10.1098/rsta.2014.0159
5. Collins, C.O., Rogers, W.E., Marchenko, A. and Babanin, A.V., 2015. In Situ Measurements of an Energetic Wave Event in the Arctic Marginal Ice Zone. *Geophysical Research Letters*, 42(6), pp. 1863-1870. doi:10.1002/2015gl063063
6. McPhee, M.G., Maykut, G.A. and Morison, J.H., 1987. Dynamics and Thermodynamics of the Ice/Upper Ocean System in the Marginal Ice Zone of the Greenland Sea. *Journal of Geophysical Research: Oceans*, 92(C7), pp. 7017-7031. doi:10.1029/jc092ic07p07017

7. Ginsburg, A.I. and Fedorov, K.N., 1989. On the Multitude of Forms of Coherent Motions in Marginal ICE Zones (MIZ). In: J. C. J. Nihoul and B. M. Jamart, eds., 1989. *Mesoscale/Synoptic Coherent Structures in Geophysical Turbulence*. Elsevier Oceanography Series, vol. 50. Amsterdam: Elsevier B.V., pp. 25-39. doi:10.1016/s0422-9894(08)70175-2
8. Ivanov, V.V., Alekseyev, V.A. and Repina, I.A., 2014. [The Increasing Impact of Atlantic Waters on the Ice Cover of the Arctic Ocean]. In: *The International Conference dedicated to the memory of academician A. M. Obukhov "Turbulence, Atmosphere and Climate Dynamics". 13-16 May 2013. Abstracts. Moscow, 13-16 May 2013*. Moscow: GEOS, pp. 336-344 (in Russian).
9. Selivanova, J.V., Tilinina, N.D., Gulev, S.K., and Dobrolubov, S.A. 2016. Impact of Ice Cover in the Arctic on Ocean-Atmosphere Turbulent Heat Fluxes. *Oceanology*, 56(1), pp. 14-18. doi:10.1134/S0001437016010185
10. Kędra, M., Moritz, C., Choy, E.S., David, C., Degen, R., Duerksen, S., Ellingsen, I., Gorska, B., Grebmeier, J.M. [et al.], 2015. Status and Trends in the Structure of Arctic Benthic Food Webs. *Polar Research*, 34(1), 23775. doi:10.3402/polar.v34.23775
11. Makarevich, P.R. and Oleinik, A.A., 2017. Barents Sea Phytoplankton during Springtime: Composition and Structure at the Sea Ice Edge. *Transactions of the Kola Science Centre*, 8(2-4), pp. 50-58. Available at: http://www.mmbi.info/fs/files/1290/Okeanologiya_vyp_4_trudy_2_17.pdf [Accessed: 04 April 2022] (in Russian).
12. Van Aken, H.M., Budéus, G. and Hähnel, M., 1995. The Anatomy of the Arctic Frontal Zone in the Greenland Sea. *Journal of Geophysical Research: Oceans*, 100(C8), pp. 15999-16014. doi:10.1029/95jc01176
13. Rodionov, V.B. and Kostianoy, A.G., 1998. *Oceanic Fronts of the Seas of the North-European Basin Seas*. Moscow: GEOS, 292 p. (in Russian).
14. Konik, A.A., Zimin, A.V. and Atadzhanova, O.A., 2019. Quantitative Estimations of the Variability of Characteristics of the Temperature of the Sea Surface in the Front of the Frontal Zone of the Kara Sea. *Fundamental and Applied Hydrophysics*, 12(1), pp. 54-61. doi:10.7868/S2073667319010076 (in Russian).
15. Brenner, S., Rainville, L., Thomson, J. and Lee, C., 2020. The Evolution of a Shallow Front in the Arctic Marginal Ice Zone. *Elementa: Science of the Anthropocene*, 8, 17. doi:10.1525/elementa.413
16. Moiseev, D.V. and Zhichkin, A.P., 2017. Thermohaline Conditions of Ice Edge Area in the Northern Barents Sea in April 2016. *Transactions of the Kola Science Centre*, 8(2-4), pp. 10-25. Available at: http://www.mmbi.info/fs/files/1290/Okeanologiya_vyp_4_trudy_2_17.pdf [Accessed: 04 April 2022] (in Russian).
17. Atadzhanova, O.A. and Zimin, A.V., 2019. Analysis of the Characteristics of the Submesoscale Eddy Manifestations in the Barents, the Kara and the White Seas Using Satellite Data. *Fundamental and Applied Hydrophysics*, 12(3), pp. 36-45. doi:10.7868/S2073667319030055

18. Liu, Y. and Minnett, P.J., 2016. Sampling Errors in Satellite-Derived Infrared Sea-Surface Temperatures. Part I: Global and Regional MODIS Fields. *Remote Sensing of Environment*, 177, pp. 48-64. doi:10.1016/j.rse.2016.02.026
19. Ivshin, V.A., Trofimov, A.G. and Titov, O.V., 2019. Barents Sea Thermal Frontal Zones in 1960–2017: Variability, Weakening, Shifting. *ICES Journal of Marine Science*, 76(suppl. 1), pp. i3-i9. doi:10.1093/icesjms/fsz159
20. Spreen, G., Kaleschke, L. and Heygster, G., 2008. Sea Ice Remote Sensing Using AMSR-E 89-GHz Channels. *Journal of Geophysical Research: Oceans*, 113(C2), C02S03. doi:10.1029/2005JC003384
21. Nesterov, E.S., 2013. *North Atlantic Oscillation: Atmosphere and Ocean*. Moscow: Triada Ltd., 144 p. (in Russian).
22. Osadchiv, A.A., 2021. *River Plumes*. Moscow: Scientific World, 284 p. (in Russian).
23. Johannessen, O.M. and Foster, L.A., 1978. A Note on the Topographically Controlled Oceanic Polar Front in the Barents Sea. *Journal of Geophysical Research: Oceans*, 83(C9), pp. 4567-4571. doi:10.1029/jc083ic09p04567
24. Pavlov, V.K. and Pfirman, S.L., 1995. Hydrographic Structure and Variability of the Kara Sea: Implications for Pollutant Distribution. *Deep Sea Research Part II: Topical Studies in Oceanography*, 42(6), pp. 1369-1390. doi:10.1016/0967-0645(95)00046-1
25. Harris, C.L., Plueddemann, A.J. and Gawarkiewicz, G.G., 1998. Water Mass Distribution and Polar Front Structure in the Western Barents Sea. *Journal of Geophysical Research: Oceans*, 103(C2), pp. 2905-2917. doi:10.1029/97jc02790
26. Bauch, D. and Cherniavskaia, E., 2018. Water Mass Classification on a Highly Variable Arctic Shelf Region: Origin of Laptev Sea Water Masses and Implications for the Nutrient Budget. *Journal of Geophysical Research: Oceans*, 123(3), pp. 1896-1906. doi:10.1002/2017jc013524

About the authors:

Aleksandr A. Konik, Junior Research Associate, P.P. Shirshov Institute of Oceanology of RAS (30, 1st Line of Vasilyevsky Island, St. Petersburg, Russian Federation, 119053); 3rd year postgraduate student of Saint-Petersburg State University (7/9 Universitetskaya Naberezhnaya, St. Petersburg, Russian Federation, 199034), **WoS ResearcherID: AAB-7195-2020**, **ORCID ID: 0000-0002-2089-158X**, **Scopus Author ID: 57203864647**, konikrshu@gmail.com

Aleksey V. Zimin, Chief Research Associate, P.P. Shirshov Institute of Oceanology of RAS (30, 1st Line of Vasilyevsky Island, St. Petersburg, 119053, Russian Federation), Dr.Sci. (Geogr.); Professor of Saint-Petersburg State University (7/9 Universitetskaya Naberezhnaya, St. Petersburg, 199034, Russian Federation), **WoS ResearcherID: C-5885-2014**, **Scopus Author ID: 55032301400**, zimin2@mail.ru

Contribution of the co-authors:

Aleksandr A. Konik – data collection and systematization; selection and analysis of literature; preparation of the article text; creation of figures

Aleksey V. Zimin – selection and analysis of literature; scientific supervision; critical analysis and revision of the text

The authors have read and approved the final manuscript.

The authors declare that they have no conflict of interest.